

## Depth Dependence of the Photoelectron Emission Profile for Cathode Lens Microscopy

Yen Huang<sup>1,2</sup>, Tzu-Hung Chuang<sup>2</sup>, Chun-I Lu<sup>2</sup>, Chih-Heng Huang<sup>3</sup>, Deng-Sung Lin<sup>1,4</sup>, Chien-Chen Kuo<sup>3</sup>, and Der-Hsin Wei<sup>1,2,3</sup>

<sup>1</sup>. Graduate Program of Science and Technology of Synchrotron Light Source, National Tsing Hua University, Hsinchu, Taiwan.

<sup>2</sup>. National Synchrotron Radiation Research Center, Hsinchu, Taiwan.

<sup>3</sup>. Program of Synchrotron Radiation and Neutron Beam Applications, National Sun Yat-sen University, Kaohsiung, Taiwan.

<sup>4</sup>. Department of Physics, National Tsing Hua University, Hsinchu, Taiwan.

\* Corresponding author, [dhw@nsrrc.org.tw](mailto:dhw@nsrrc.org.tw)

Photoemission/low-energy electron microscope (PEEM/LEEM) records the two-dimensional (2D) electron emission maps with a beam-acceleration lens that treats the sample as a cathode. The cathode lens greatly improves the microscope's electron collection efficiency, but it comes with additional aberrations that are hard to compensate even with a state-of-the-art aberration corrector [1]. Another uncorrectable image degradation in PEEM is the space charge effects triggered by intense pulsed photon illumination [2]. In this report, we look into another fundamental constraint when X-ray excited electrons are collected to image the objects buried underneath specimen's surface. Because X-ray's attenuation length is longer than the low-energy electron's inelastic mean free path (IMFP) in general, it is straightforward to identify the player who is responsible for the limited probing depth in photoelectron detection. It is less obvious however to foresee of what probabilities and at what location that the electrons emitted from a distance  $d$  inside the specimen would escape the sample. This is because, as illustrated in Figure. 1, the photo-excited electrons emitted inside the specimen spread out in every direction and travel different distances before reaching surface. As a result, the distribution of ejected electrons is expected to vary with the depth where original emission occurred. This depth dependence has nothing to do with the acceleration field applied in cathode lens nor the space charge effects.

Our study begins with two assumptions to simplify the calculation; one is the isotropic emission of photo-excited electrons, the other is that every photo-excited electron runs a straight line trajectory with an IMFP-weighted intensity. Only those electrons with their elevation angles lying between 0 - 180 degree are taken into consideration in our code (C language). Three more physical quantities are implemented in the code; energy dependent IMFP following the universal curve [3], work function of the surface, and the conservation of momentum parallel to surface. Following the first assumption, we set up multiple emission events from the buried object. The second assumption allows us to track the trajectory of each given photo-excited electron; from its emission to its impact at surface. The inclusion of IMFP-weighted intensity is to estimate the intensity loss related to the inelastic/elastic scattering. Finally, the work function and momentum conservation are used to discriminate those electrons which have inadequate kinetic energy or incident angle to break free from surface. Figure 2 displays our calculation results for a 5 nm wide object buried at three different depths; 1nm, 3nm, and 5nm. Considering the PEEM lens is rotational symmetric along its optical axis, we only calculate the trajectories on x-z plane, where z-axis is the surface normal aligning to the optical axis of the PEEM lens. Figure 2 are the electron emission profiles calculated with electrons flying with a 10 eV kinetic energy inside a metal of 5 eV surface work function. The numerical values chosen here are to simplify our model calculation, and the IMFP,  $\lambda$ , of an electron

carrying the kinetic energy of  $E$  is estimated by the equation  $\lambda = 143/E^2 + 0.054(E)^{1/2}$  [3]. The numerical conclusion drawn below is expected to vary slightly if a different equation is used to evaluate  $\lambda$ .

According to the electron intensity versus position plots shown in Figure 2, the electron intensity profiles at the surface are sensitive to the depth where the object is buried. A buried depth varying from 1 nm to 5 nm changes the full width at half maximum (FWHM) of the profile from 5 nm to 6.5 nm. At the meantime, the distance corresponding to 10/90 knife-edge changes from 1.4 nm to 4.4 nm. This finding suggest, even with a perfect lens, the image resolution of an object buried at a distance of 5 nm beneath surface can at best be 4.4 nm, providing 5 eV of electrons (after overcoming the surface work function) are collected for imaging. Results displayed in Figure 2 also reveal that the electron intensity profile would get weaker and look more blurred as the object is buried deeper inside the specimen. We note here that the calculation shown here is performed with a single kinetic energy. In reality, when secondary electrons are collected for imaging, summation of multiple profiles will be needed to evaluate the impacts of electron energy spread. For PEEM collecting high energy core electrons (a few keV) [4], we expect the electron intensity profile on surface would depend less on emission depth due to the longer IMFP exhibited by high energy electrons.

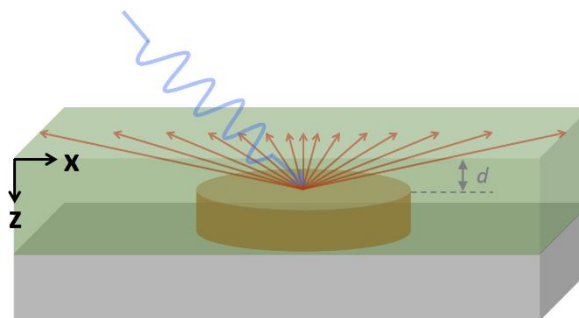


**Figure 1.** X-ray excited electrons emitted from an object buried at a depth of  $d$  create an electron emission profile on surface.

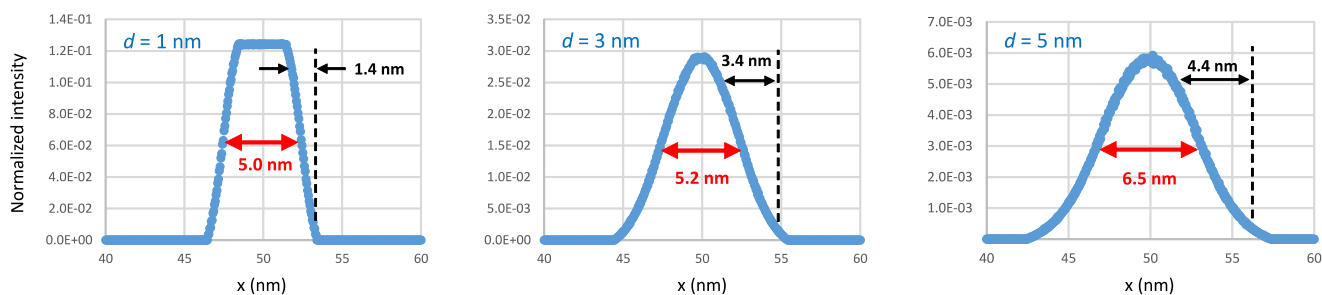


**Figure 2.** Profiles of photo-excited electron appeared at surface after emitting from a distance  $d$  beneath the surface. The test object is 5 nm wide, placed at location  $x = 47.5$  to  $52.5$  nm. The electron intensities at surface are normalized to that emitted at  $d = 0$ . FWHM and knife-edge of electron intensity profile show significant depth dependence. The IMFP used for 10 eV electron is

#### References:

- [1] J. Feng *et al*, *J. Phys.: Condensed Matter* **17** (2005), S1339.
- [2] Th. Schmidt *et al*, *Ultramicroscopy* **126** (2013), 23.
- [3] M. P. Seah and W. A. Dench, *Surf. Interface Anal.* **1** (1979), 2.
- [4] M. Patt *et al*, *Rev. Sci. Instrum.* **85** (2014), 113704.